Dynamics of wave packets in two-dimensional random systems with anisotropic disorder

Gregory Samelsohn* and Eugene Gruzdev
Department of Communication Engineering, Holon Institute of Technology, Holon 58102, Israel
(Received 7 April 2008; published 3 September 2008)

A theoretical model is proposed to describe narrowband pulse dynamics in two-dimensional systems with arbitrary correlated disorder. In anisotropic systems with elongated cigarlike inhomogeneities, fast propagation is predicted in the direction across the structure where the wave is exponentially localized and tunneling of evanescent modes plays a dominant role in typical realizations. Along the structure, where the wave is channeled as in a waveguide, the motion of the wave energy is relatively slow. Numerical simulations performed for ultra-wide-band pulses show that even at the initial stage of wave evolution, the radiation diffuses predominantly in the direction along the major axis of the correlation ellipse. Spectral analysis of the results relates the long tail of the wave observed in the transverse direction to a number of frequency domain "lucky shots" associated with the long-living resonant modes localized inside the sample.

DOI: 10.1103/PhysRevE.78.036601 PACS number(s): 41.20.Jb, 42.25.Dd, 43.20.+g

I. INTRODUCTION

Propagation of waves in two-dimensional (2D) random media has some specific features that make it rather different from that observed in their three-dimensional counterparts. It is believed generally that in 2D, the wave is always localized irrespective of the disorder strength, in contrast to 3D structures, where a certain amount of disorder is needed for the localization set up [1].

Two-dimensional systems demonstrating Anderson localization are widespread in both classical and quantum physics. For example, measurements of microwave radiation localized by scattering from a random array of dielectric cylinders placed between a pair of parallel conducting plates were reported in [2]. Although coupled with radiation modes, plasmons are also shown to be localized on a rough metallic surface [3]. The analogous effect is also evident for elastic waves in randomly loaded membranes [4] and surface waves on a rough bottom. An experimental demonstration of the latter was carried out in a rather exotic system, namely, by studying the propagation of third sound waves on superfluid helium adsorbed to a 2D disordered substrate [5]. Observation of strong localization has been performed recently for light propagating along 2D highly disordered photonic lattices [6], the first practical realization of the transverse localization concept [7]. Anderson localization is also an intrinsic feature for a variety of 2D electron gas systems where disorder prevails over the interactions, including doped semiconductors [8] and disordered superconductors [9], to name a few. The results of the recently published calculations suggest that the Anderson localization of cold atoms [10] or Bogolyubov quasiparticles in Bose-Einstein condensates could be possible under experimentally accessible conditions [11].

The mathematical definition of localization usually refers to an *infinite system*, in which there are only localized states [12], i.e., the eigenfunctions of the wave operator decrease exponentially at infinity, $\psi_i(\mathbf{r}) \propto \exp[-(\mathbf{r}-\mathbf{r}_i)/2\xi]$. The damping rate of these localized modes (more correctly, of their envelope squared), the so-called inverse localization length $\xi^{-1}(\mathbf{k})$, should depend somehow on the wave vector $\mathbf{k}$ and the statistics of the scattering potential. However, it is much more important in practice that the presence of wave localization alters dramatically the wave transport through *finite systems* with open boundaries [13]. For example, in a slab geometry, the intensity of the transmitted wave decreases exponentially with the slab width L, i.e., in typical realizations $I(L) \propto \exp[-L/\xi(k)]$, instead of the $1/L$ dependence predicted by the classical diffusion theory.

The issue of wave localization in random media with anisotropic disorder is still controversial. By such a disorder, we mean that the relevant constitutive parameter, say, dielectric permittivity $\varepsilon(\mathbf{r})$, is assumed to be a scalar value, but its correlation function $B_\varepsilon(\mathbf{r})=\langle\varepsilon(\mathbf{r}')\varepsilon(\mathbf{r}'+\mathbf{r})\rangle$ is allowed to be anisotropic. In geophysics, for instance, the typical horizontal scale of many natural media is usually much larger than the vertical one, so that the correlation ellipsoid has a pancakelike form. A variety of photonic or electronic materials of interest to modern technologies are also characterized by a highly anisotropic microstructure. Most of the related theoretical results published in the literature are based on an anisotropic tight-binding Hamiltonian that can be mapped onto a network model; both formulations assume the disorder is of a short-range type (δ correlated in space). The results of these studies indicate, in particular, that in 2D the wave is completely localized irrespective of the anisotropy level, but the localization length depends on the direction of wave propagation [14–16].

Random media are not simply a limiting form of chaos like a white noise, but instead have some structure that becomes apparent in correlation functions of their constitutive parameters. Random composites like ceramics or heterogeneous polymer phases, polycrystals and foams, colloids, granular media, and biological tissues demonstrate *long-range correlations*, sometimes of rather sophisticated form, e.g., multifractal. The model of δ-correlated potential may be relevant for electron waves scattered by lattices with pointlike impurities in the long-wavelength limit. However, this model is surely not applicable to the most interesting resonant regime of classical waves propagating in continuous

*samelsohn@hit.ac.il.

media where the wavelength is comparable to the correlation scale of the disorder. As we have shown recently for the long-range correlated disorder, the transport properties of continuous random media seem to be essentially different in the directions along and across the major axis of the correlation ellipse, at least for a weak scattering in the resonant regime [17,18]. In particular, it was demonstrated that there exists a frequency-dependent critical value of the anisotropy parameter below which waves are localized at all angles of propagation. Above this critical value, the radiation is localized only within some angular sectors centered at the short axis of the correlation ellipse and is extended in other directions.

In the present paper, we continue these works by addressing the problem of *time-domain* wave transport of narrowband wave packets in 2D systems. Two fundamental issues are considered here: First, how the localization affects the dynamics of pulsed waves propagating through statistically isotropic 2D media (see also the results of calculations with 2D discrete models [19–21], and a theoretical analysis [22] and experimental work [23] both concerning wave propagation in 3D samples); and second, whether the temporal behavior of the wave can be altered essentially when the disorder becomes anisotropic. Using the simplest perturbative model yet capturing the essential physics, we can also answer the central question that has been largely ignored in the previous studies. Specifically, we explore a relationship between the relevant quantity (such as delay time for dynamic measurements), on the one hand, and the correlation properties of the scattering potential, on the other.

II. COHERENCE FUNCTION

Confining ourselves to exploring the scalar classical waves, we start with the Green's function,

$$G_\omega(\mathbf{r}) = \frac{i}{2k}\int_0^\infty d\tau \exp(ik\tau/2)\int D\mathbf{v}(t)\,\delta\left[\mathbf{r} - \int_0^\tau dt\mathbf{v}(t)\right] \times \exp\left\{i\frac{k}{2}\int_0^\tau dt\left[\mathbf{v}^2(t) + \tilde{\varepsilon}\left(\int_0^t dt'\mathbf{v}(t')\right)\right]\right\}, \quad (1)$$

written in a so-called velocity (or white-noise) representation of the Feynman path integral for a time harmonic source, where $\delta(\cdot)$ is the Dirac δ function, ω stands for the angular frequency of the radiation, and $k=\omega/c$ is the wave number in a homogeneous reference medium characterized by the wave velocity c. Here, it is assumed that k contains an (infinitesimally small) positive imaginary part that enforces the radiation condition at infinity and provides the convergence of the corresponding integral. Perturbation $\tilde{\varepsilon}(\mathbf{r})$ entering Eq. (1) and playing the role of a scattering potential is a zero mean random field. The basic quantity we evaluate here is the two-frequency mutual coherence function (frequency field-field correlator) defined as

$$\Gamma(\omega,\Omega) = \langle G_{\omega+\Omega/2}G^*_{\omega-\Omega/2}\rangle, \quad (2)$$

which is an important quantity in itself, but primarily due to the fact that being properly normalized,

$$\tilde{\Gamma}(\omega,\Omega) = \Gamma(\omega,\Omega)/\Gamma(\omega,0), \quad (3)$$

and then Fourier transformed, it gives the impulse response function (photon time-of-flight distribution),

$$J(\omega,t) = \frac{1}{2\pi}\int_{-\infty}^{\infty} d\Omega \exp(-i\Omega t)\tilde{\Gamma}(\omega,\Omega), \quad (4)$$

for a narrowband pulse with spectrum centered around a given frequency ω as, e.g., for a picosecond duration pulse of visible light. Note that the impulse response function satisfies the natural normalization condition $\int dtJ(\omega,t)=1$.

To evaluate the coherence function, we first rescale the integration paths in the corresponding Green's functions as $\mathbf{v}_n(t)\rightarrow\alpha_n\mathbf{v}_n(t)$, where the coefficients α_n are given by $\alpha_n=\sqrt{k/k_n}$ (here $n=1,2$), and $k\equiv k(\omega)$ is the wave number corresponding to a "central" frequency ω. Then, introducing the Wigner-type functional variables,

$$\mathbf{w}(t) = \frac{1}{2}[\mathbf{v}_1(t) + \mathbf{v}_2(t)], \quad \mathbf{v}(t) = \mathbf{v}_1(t) - \mathbf{v}_2(t), \quad (5)$$

we substitute Eq. (1) into Eq. (2) and perform ensemble averaging. In order to dispose of the integrals over pseudotime, an asymptotic procedure resembling the classical method of stationary phase is used [24]. Then, the normalized correlator in an m-dimensional system is presented as a double path integral of the form

$$\begin{aligned}\tilde{\Gamma}(\omega,\Omega) \simeq{}& \tilde{\Gamma}_0(\omega,\Omega)(\alpha_1\alpha_2)^{-m}\int D\mathbf{w}(t)\int D\mathbf{v}(t)\\ &\times\delta\left[(\alpha_1+\alpha_2)\eta\mathbf{r}/2 - \int_0^L dt\mathbf{w}(t)\right]\\ &\times\delta\left[(\alpha_1-\alpha_2)\eta\mathbf{r} + \int_0^L dt\mathbf{v}(t)\right]\\ &\times\exp\left[ik\int_0^L dt\mathbf{w}(t)\cdot\mathbf{v}(t)\right]\\ &\times\exp\{-\tilde{X}[\mathbf{w}(t),\mathbf{v}(t);\omega,\Omega]\}, \end{aligned} \quad (6)$$

where $\tilde{\Gamma}_0(\omega,\Omega)$ is the normalized coherence function in a homogeneous reference medium, L is the distance between the source and the observation point,

$$\tilde{X}[\mathbf{w}(t),\mathbf{v}(t);\omega,\Omega] = X[\mathbf{w}(t),\mathbf{v}(t);\omega,\Omega] - X[\mathbf{w}(t),\mathbf{v}(t);\omega,0], \quad (7)$$

and the functional X, in its turn, is given by

$$\begin{aligned}X[\mathbf{w}(t),\mathbf{v}(t);\omega,\Omega] ={}& \frac{k^2}{8}\int_0^L dt_1\int_0^L dt_2\\ &\times\{\alpha_1^{-4}B_\varepsilon[\mathbf{r}_1(t_1)-\mathbf{r}_1(t_2);\omega_1,0]\\ &-2(\alpha_1\alpha_2)^{-2}B_\varepsilon[\mathbf{r}_1(t_1)-\mathbf{r}_2(t_2);\omega,\Omega]\\ &+\alpha_2^{-4}B_\varepsilon[\mathbf{r}_2(t_1)-\mathbf{r}_2(t_2);\omega_2,0]\}\end{aligned} \quad (8)$$

(here the additional arguments in the correlation functions take into account an arbitrary permittivity dispersion of the medium). The functional paths entering Eq. (8) are written as

$$\mathbf{r}_1(t) = \alpha_1 \int_0^t dt[\mathbf{w}(t) + \mathbf{v}(t)/2], \tag{9a}$$

$$\mathbf{r}_2(t) = \alpha_2 \int_0^t dt[\mathbf{w}(t) - \mathbf{v}(t)/2]. \tag{9b}$$

The double path integral in Eq. (6) may be evaluated by applying a cumulant technique [17]. This results in

$$\tilde{\Gamma}(\omega,\Omega) = \tilde{\Gamma}_0(\omega,\Omega)\exp[-\tilde{\chi}(\omega,\Omega)], \tag{10}$$

where $\tilde{\chi}(\omega,\Omega)$ is, generally, the cumulant series which, for nondispersive media, is approximated here by the first cumulant (see Ref. [24] for technical details),

$$\tilde{\chi}(\omega,\Omega) = \frac{\pi}{2}k^3 L \int d\mathbf{K}\tilde{f}(\mathbf{K},\omega,\Omega)\mathbf{\Phi}_\varepsilon(\mathbf{K}), \tag{11}$$

and $\Phi_\varepsilon(\mathbf{K})$ is the power spectrum of the disordered system, i.e., Fourier transform of the pair correlation function $B_\varepsilon(\mathbf{r})$. The kernel of the integral transform (11), called the (normalized) filtering function in our previous works [17,18], has the form

$$\tilde{f}(\mathbf{K},\omega,\Omega) = K^{-2}\{1 - \exp[i\Omega L(K/8ck^2)(K - 2\mathbf{k}\cdot\mathbf{K}/K)]\} \times \vartheta(K - |2\mathbf{k}\cdot\mathbf{K}/K|), \tag{12}$$

where $\vartheta(\cdot)$ is the Heaviside step function. The wave vector $\mathbf{k}$ is directed along the line connecting the source with the observation point, its length being equal to k. As follows from Eq. (12), the loss of coherence between two waves with different frequencies is due to both Bragg scattering on spectral components lying within the limiting sphere of the Ewald construction ($K \leqslant 2k$) and also to local high-frequency resonances ($K > 2k$); see Fig. 1.

Another issue that can be covered by using our model of the coherence function is the role of dissipation. In an absorptive medium, the dissipation is usually accounted for by taking the scattering potential (permittivity or refractive index) to be a complex-valued field. When the dissipation is small, a possible alternative is to consider the scattering potential to be real while assigning a small imaginary part to the frequency or wave number: $k \to k + i\gamma$, where γ is the decrement of the field in a homogeneous medium. Without scattering, the intensity of the wave will then decrease as $\exp(-2\gamma L)$, the factor that has to be included in the expression for $\Gamma_0(\omega,\Omega)$. Interaction of scattering and absorption is determined by the cumulant $\tilde{\chi}(\omega,\Omega)$ in which the substitution $\Omega \to \Omega + 2ic\gamma$ should be performed [24].

III. DIFFUSE TIME

In studying wave-packet dynamics, we consider only the first temporal moment of $J(\omega,t)$, namely the mean arrival time (also known as delay, diffuse, or traversal time) defined as [25]

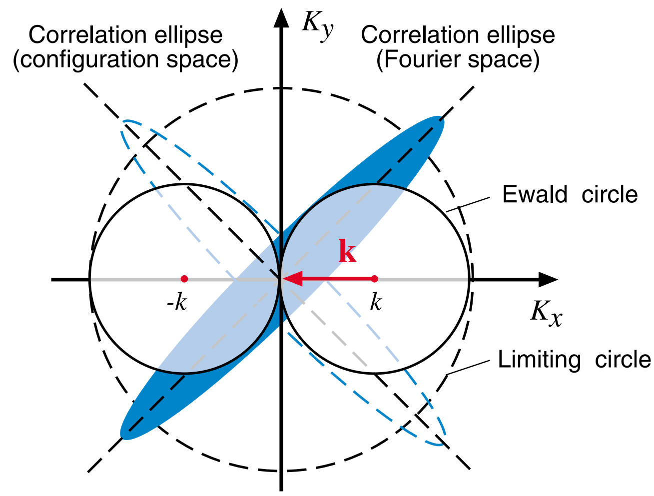

FIG. 1. (Color online) Two-dimensional version of the Ewald construction. The points of the Ewald sphere for a given wave vector **k** determine all possible spectral components that could resonantly transform the incident wave into a scattered one. The limiting sphere encircles all spectral components coupling any two wave vectors in the process of elastic scattering. An example of the correlation ellipse for a medium with elongated cigarlike inhomogeneities is shown in both configuration and Fourier space. The major axis of the ellipse in configuration space corresponds to the direction of higher correlation.

$$\tau(\mathbf{k}) = \int_{-\infty}^{\infty} dt t J(\omega,t), \tag{13}$$

where the argument of τ is intended to stress the fact that in the general case, the delay time should depend upon both modulus and direction of the wave vector $\mathbf{k}$ [note that such dependence is demonstrated explicitly by the coherence function, Eqs. (10)–(12) and then has to be present in the impulse response]. Substituting Eq. (3) into this definition, interchanging the integration order, and identifying the integral over t with the first derivative of the δ function, we obtain

$$\tau(\mathbf{k}) = i \left.\frac{\partial\tilde{\Gamma}(\omega,\Omega)}{\partial\Omega}\right|_{\Omega=0}. \tag{14}$$

Hence we find that $\tau(\mathbf{k}) = \tau_0 + \tilde{\tau}(\mathbf{k})$, i.e., the delay time is composed of the time of propagation in a homogeneous reference medium $\tau_0 = L/c$, the term originating from $\tilde{\Gamma}_0(\omega,\Omega)$, and the excess delay time $\tilde{\tau}(\mathbf{k}) = i\tilde{\chi}'(\omega,0)$, related to the photon random walk and arising from the corresponding exponential in Eq. (10). Thus, performing the required differentiation for nondissipative media ($\gamma=0$), we arrive at

$$\tilde{\tau}(\mathbf{k}) = \frac{\pi k L^2}{16c}\int d\mathbf{K}\,\vartheta(K - |2\mathbf{k}\cdot\mathbf{K}/K|)\mathbf{\Phi}_\varepsilon(\mathbf{K}). \tag{15}$$

Always taking only positive values, the model obtained satisfies the causality principle. The final result, which is valid for both two- and three-dimensional systems, is formulated as a transformation of the classical integral geometry: to find the delay time, we should integrate the power spectrum over the visible area, i.e., just outside the eight curve formed by the two Ewald spheres; see Fig. 1. Moreover, it can be shown that the integral transform (15) is invertible, which allows one, in principle, to reconstruct the power spectrum of a heterogeneous medium by measuring the angular distributions of the diffuse time for pulsed waves of different frequencies [26].

Although our perturbative model for the coherence function is not so accurate deep in the diffusion regime (mainly by virtue of the fact that only the first cumulant is taken into account), its first temporal moment, $\bar{\tau}(\mathbf{k})$, is reliable under all possible propagation conditions. Indeed, as can be shown by expanding the functional $\tilde{X}(\omega,\Omega)$ into a Taylor series at $\Omega=0$, the contribution of all higher cumulants to the first derivative of $\tilde{\chi}(\omega,\Omega)$ is exactly zero.

It is worth noting that our starting formulation deals with the point source located in an infinite medium. However, an absorption [let us recall that the wave number in Eq. (1) has a positive imaginary part] or, equivalently, some leakage at the boundaries, though located arbitrarily far from the source, is implicitly assumed to ensure the convergence of the corresponding integrals and to prevent any singularities that are possible in unbounded media with localization. Another effect is related to the stationary phase approximation we use on the way to Eq. (6), also eliminating effectively the contribution of wave scattering from distant areas of the medium to the measured field. Overall, this makes our geometry much more similar to that of a finite sample with open boundaries. It has been instructive, therefore, to test the delay time $\bar{\tau}(k)$ calculated for isotropic 3D media against the results of the measurements performed for ultrasound [27], microwaves [23,28], and optical waves [29] diffused through a slab of a strongly scattering medium. The theoretical predictions appear to be of the same order of magnitude as the corresponding measured values, a rather surprising coincidence by virtue of the fact that in all these experiments, the radiation is of a vector nature, in contrast to the scalar model adopted here.

In principle, our main goal here is to explore the effect of microstructure, which is assumed to be universal, uncoupled in a sense from the details of the sample's geometry. In what follows, we consider 2D systems. As an example, we assume that the medium is described by an anisotropic Gaussian correlation function,

$$B_\varepsilon(\mathbf{r}) = \sigma_\varepsilon^2 \exp(-\mu x^2/\ell_\varepsilon^2 - y^2/\mu\ell_\varepsilon^2), \tag{16}$$

where σ_ε^2 is the variance of the fluctuations, while ℓ_ε and μ are, respectively, the mean geometrical value and the ratio of the correlation lengths along the two coordinate axes (see Fig. 2). When, for instance, $\mu>1$, the inhomogeneities are stretched along the y axis. Since the two situations, $\mu>1$ and $\mu<1$, are topologically equivalent, we consider only the case $\mu>1$. The value of μ defined in this manner is therefore the inverse of the aspect ratio.

Substituting the corresponding expression for the power spectrum $\Phi_\varepsilon(\mathbf{K})$ into Eq. (10) and performing integration over the radial coordinate leads to

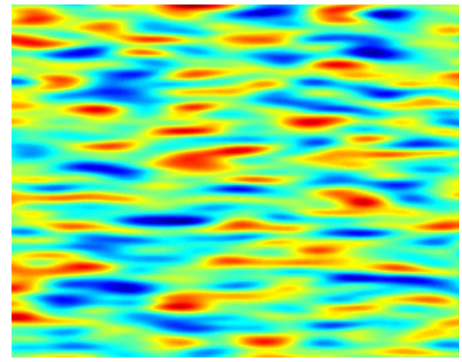

FIG. 2. (Color online) Realization of the scattering potential with Gaussian correlation function, Eq. (16). Random medium is modeled by Fourier transforming a two-dimensional $\mathbf{K}$-space white noise sample multiplied by $\sqrt{\Phi_\varepsilon(\mathbf{K})}$. The inhomogeneities are stretched in the horizontal direction, $\mu=8$.

$$\bar{\tau}(\boldsymbol{\kappa}) = T\frac{\kappa}{\sqrt{\pi}}\int_0^\pi d\phi' a_\mu^{-2}(\phi')\exp[-a_\mu^2(\phi')\cos^2(\phi-\phi')\kappa^2], \tag{17}$$

where

$$a_\mu^2(\phi) = \mu \sin^2\phi + (1/\mu)\cos^2\phi, \tag{18}$$

$\kappa=kl_\varepsilon$ is the normalized wave number, ϕ is the angle measured between the short axis of the correlation ellipse and the direction of wave propagation, and $T=\sqrt{\pi}\sigma_\varepsilon^2L^2/32c\ell_\varepsilon$ is the isotropic high-frequency delay (see below). In statistically isotropic media, the remaining integration may be performed analytically, which results in

$$\bar{\tau}(\kappa) = T\sqrt{\pi}\kappa\exp(-\kappa^2/2)I_0(\kappa^2/2), \tag{19}$$

where $I_0(\cdot)$ is the modified Bessel function of the first kind. As follows from the latter equation, the delay time increases linearly with κ in the long-wavelength regime $(\kappa\ll1)$, reaches its maximum value $\sim1.18T$ at $\kappa\simeq1$, and then decreases slightly by approaching T in the high-frequency limit $(\kappa\gg1)$. Qualitatively, this behavior is similar to that demonstrated by the inverse localization length $\xi^{-1}(\kappa)$ in isotropic 2D media, although the latter quantity has a more pronounced maximum in the resonant regime [17].

In the long-wavelength limit, $\mu\kappa^2\ll1$, the transport dynamics remains isotropic even for anisotropic systems. Geometrically, the correlation ellipse in the Fourier space is much greater in size than the Ewald circles, and their rotations cut out only a very small part of the power spectrum, hardly influencing the result of integration. In contrast, anisotropic systems in the resonant $(\kappa\sim1)$ and high-frequency regimes do alter essentially the wave-packet dynamics by redistributing the energy flow between different directions. As is seen from Fig. 3, the diffuse time is always smaller in the direction across $(\phi=0°,180°)$ than in the direction along $(\phi=\pm90°)$ the structure.

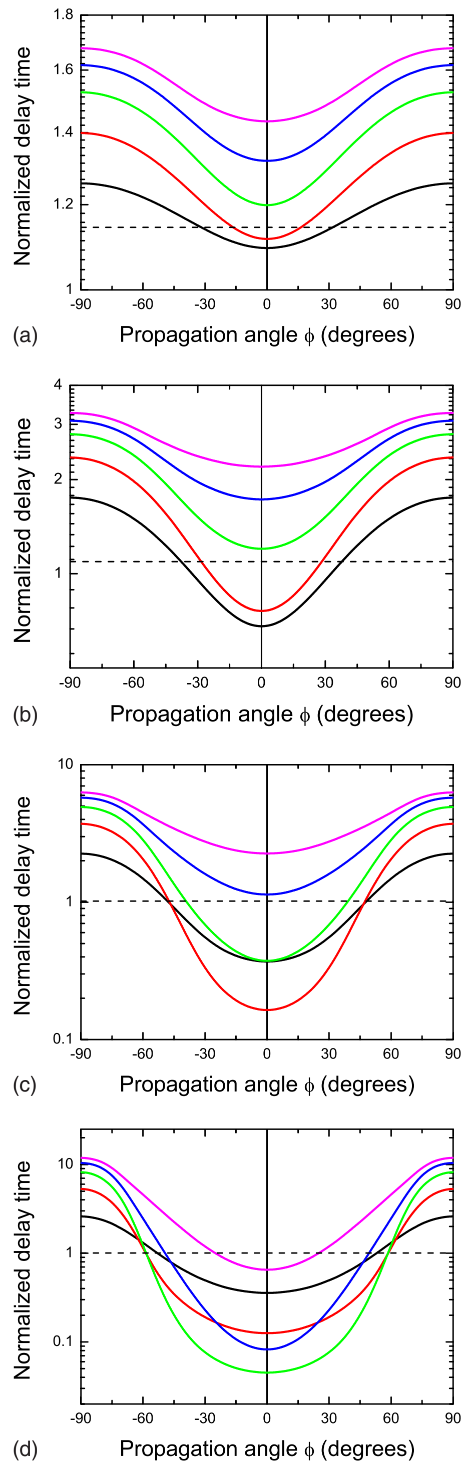

FIG. 3. (Color online) Delay time $\tilde{\tau}$ calculated as a function of propagation angle ϕ for a number of different values of the normalized wave number κ: (a) $\kappa=1$, (b) $\kappa=2$, (c) $\kappa=4$, (d) $\kappa=8$. The dashed line indicates the isotropic case ($\mu=1$). Other curves correspond to $\mu=2$, 4, 8, 16, and 32; delay time increases monotonically with μ in the direction along the structure ($\phi=\pm 90°$).

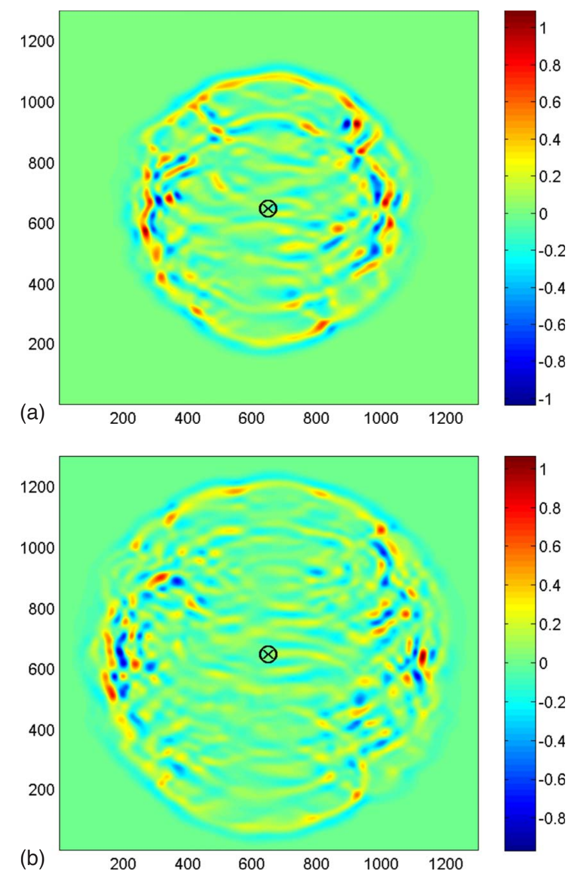

FIG. 4. (Color online) Two consecutive snapshots of an electromagnetic pulsed wave (TM mode) propagating in a randomly varying dielectric medium that is constant in the transverse direction. Numerical simulations are performed using the finite-difference time-domain technique, supplemented by absorbing boundary conditions. A very short pulse (first derivative of the Blackman-Harris waveform) with overall 310 time steps duration is radiated by a point source located at the center (labeled by the ⊗ sign) of the computation domain. Spatial electric field distribution is registered at (a) $t=1500$ and (b) $t=1900$ time steps. The statistics of random dielectric structure is exactly the same as in Fig. 2, with the following set of related parameters: $\langle\varepsilon\rangle=4$, $\sigma_\varepsilon^2=1$, and $\ell_\varepsilon=30$ grid points. Inhomogeneities of the medium are stretched in the horizontal direction ($\mu=8$). It is seen that even at the initial stage of wave evolution, the radiation diffuses predominantly in the direction along the structure, while the propagation in the transverse direction is highly suppressed. Note a relative slowdown of the wave motion in the direction of wave channeling, and also the field fragmentation there, in contrast to a sharply defined wave front running at a maximum velocity across the structure

IV. ANALYSIS

At first glance, this result looks counterintuitive. Indeed, as follows from direct numerical simulations we have performed for ultra-wide-band pulses in open disordered systems [30], the dynamics of propagation seems to be characterized by just the inverse relation. Specifically, the tail of the pulse (or coda wave, using the geophysics terminology) scattered along the structure is typically shorter than that measured in the transverse direction. This paradox, however, may be easily resolved by inspecting the spectral content of the transmitted waves [30]. Actually, in the propagation along, almost all frequencies of the original pulse are usually present in the recorded signal. At the same time, in the propagation across, most of the spectral components are lost; only a small number of frequency domain "lucky shots" survive here, the others escape due to the radiation channeling along the structure.

These lucky shots governing the time-domain dynamics of ultra-wide-band signals are reminiscent of the localized modes causing enhanced transmission through one-dimensional disordered samples. According to the effective cavity approach [31], the random 1D medium can be replaced conceptually by a combination of two potential barriers separated by a transparent segment (a kind of quantum well) having a length that is approximately equal to the localization length ξ at the resonant frequency. Although the potential involved here is random, the essential physics is actually the same as, for example, in a resonant tunneling of electromagnetic or acoustic waves through a double barrier consisting of two photonic/phononic crystals. As has been recently shown [32], on resonance the group delay measured in such a system is large, while off resonance the wave propagation is very fast, the latter in agreement with vanishingly small tunneling time in under-the-barrier propagation of both classical and quantum-mechanical waves.

Thus, these are the high-Q long-living modes that are responsible for the long tail observed in *ultra-wide-band* measurements. It is worth noting that our theory deals with *narrowband* wave packets, hence the probability of their resonant transmission should be very low, at least for sufficiently large samples, and the contribution of these modes to the overall delay time statistics has to be negligible. The tunneling may then be considered as a dominant mechanism here, which explains the reduction of $\tilde{\tau}$ predicted by our model for waves propagating across the structure.

The question of true absence of localization along the structure as predicted in [18] remains open and deserves further analysis. In our simulations (one such example is presented in Fig. 4), consistent in general with the developed theoretical model, the size of the disordered sample is obviously much smaller than the localization length ξ in this direction, even if the localization is present. In any case, another mechanism causing a high transmission is known to exist: the so-called necklace states [33], i.e., the spectrally overlapping modes supported by a set of coupled effective cavities, observed recently in the 1D slab geometry [34]. Since the coupling between neighboring modes in the direction along the structure should be highly enhanced due to anisotropy of the medium, the increase of the delay time predicted by our model for $\phi = \pm 90°$ may find a natural explanation.

V. SUMMARY

We have developed a theoretical model describing explicitly the dynamics of narrowband wave packets in random media. The model relates the delay time to the correlation properties of the disorder through a linear integral operator, allowing a simple geometry-based analysis. The delay time in isotropic 2D systems is shown to increase linearly with frequency in the long-wavelength limit, to achieve a maximum value in the resonant regime, and to be a constant for higher frequencies. In anisotropic systems, fast propagation is predicted in the direction across the structure where the wave is localized. This behavior is associated with wave tunneling via fast evanescent modes, the mechanism providing energy transport in typical realizations. Along the structure, where the wave is channeled as in a waveguide, the motion of the wave energy is relatively slow. The question of whether this channeling is supported by true extended states or is due to the excitation of necklace modes requires further investigation. Numerical simulations of short-term dynamics of pulsed electromagnetic waves support in general the above conclusions, but cannot provide a definite answer for large systems due to computer limitations. At the same time, the related phenomena may be studied experimentally in a variety of two-dimensional systems with classical waves or quantum particles.

[1] E. Abrahams, P. W. Anderson, D. C. Licciardello, and T. V. Ramakrishnan, Phys. Rev. Lett. **42**, 673 (1979).

[2] R. Dalichaouch *et al.*, Nature **354**, 53 (1991).

[3] S. I. Bozhevolnyi, Ann. Phys. **8**, 717 (1999).

[4] L. Ye, G. Cody, M. Zhou, P. Sheng, and A. N. Norris, Phys. Rev. Lett. **69**, 3080 (1992).

[5] D. R. Luhman, J. C. Herrmann, and R. B. Hallock, Phys. Rev. Lett. **94**, 176401 (2005).

[6] T. Schwartz, G. Bartal, S. Fishman, and M. Segev, Nature **446**, 52 (2007).

[7] H. De Raedt, A. Lagendijk, and P. de Vries, Phys. Rev. Lett. **62**, 47 (1989).

[8] S. V. Kravchenko and M. P. Sarachik, Rep. Prog. Phys. **67**, 1 (2004).

[9] Y. Dubi, Y. Meir, and Y. Avishai, Nature **449**, 876 (2007).

[10] R. C. Kuhn, C. Miniatura, D. Delande, O. Sigwarth, and C. A. Müller, Phys. Rev. Lett. **95**, 250403 (2005).

[11] P. Lugan, D. Clément, P. Bouyer, A. Aspect, and L. Sanchez-Palencia, Phys. Rev. Lett. **99**, 180402 (2007).

[12] I. M. Lifshits, S. A. Gredeskul, and L. A. Pastur, *Introduction to the Theory of Disordered Systems* (Wiley, New York, 1988).

[13] B. A. van Tiggelen, in *Diffuse Waves in Complex Media*, edited by J.-P. Fouque (Kluwer, Dordrecht, 1999), pp. 1–60.

[14] P. Wölfle and R. N. Bhatt, Phys. Rev. B **30**, 3542 (1984).

[15] W. Xue, P. Sheng, Q.-J. Chu, and Z.-Q. Zhang, Phys. Rev. Lett. **63**, 2837 (1989).

[16] Q. Li, S. Katsoprinakis, E. N. Economou, and C. M. Soukoulis, Phys. Rev. B **56**, R4297 (1997).

[17] G. Samelsohn, S. A. Gredeskul, and R. Mazar, Phys. Rev. E **60**, 6081 (1999).

[18] G. Samelsohn and V. Freilikher, Phys. Rev. E **70**, 046612 (2004).

[19] R. L. Weaver, Phys. Rev. B **49**, 5881 (1994).

[20] P. Sebbah, D. Sornette, and C. Vanneste, Phys. Rev. B **48**,

12506 (1993).
[21] C. W. J. Beenakker, K. J. H. van Bemmel, and P. W. Brouwer, Phys. Rev. E **60**, R6313 (1999).
[22] S. E. Skipetrov and B. A. van Tiggelen, Phys. Rev. Lett. **96**, 043902 (2006).
[23] Z. Q. Zhang *et al.*, e-print arXiv:cond-mat/0710.3155.
[24] G. Samelsohn, V. Freilikher, and M. Haridim (unpublished).
[25] G. Samelsohn and V. Freilikher, Phys. Rev. E **65**, 046617 (2002).
[26] G. Samelsohn (unpublished).
[27] J. H. Page *et al.*, Physica B, **263-264** 37 (1999).
[28] P. Sebbah, R. Pnini, and A. Z. Genack, Phys. Rev. E **62**, 7348 (2000).
[29] I. M. Vellekoop, P. Lodahl, and A. Lagendijk, Phys. Rev. E **71**, 056604 (2005).
[30] G. Samelsohn, in *Proceedings of Metamaterials 2007*, edited by F. Bilotti and L. Vegni (University Roma Tre, Rome, 2007), pp. 25–28.
[31] K. Yu. Bliokh, Yu. P. Bliokh, and V. Freilikher, J. Opt. Soc. Am. B **21**, 113 (2004).
[32] F. Van Der Biest *et al.*, Europhys. Lett. **71**, 63 (2005).
[33] J. B. Pendry, J. Phys. C **20**, 733 (1987).
[34] J. Bertolotti, S. Gottardo, D. S. Wiersma, M. Ghulinyan, and L. Pavesi, Phys. Rev. Lett. **94**, 113903 (2005).